3-D modelling, disparity, and ecology of the first Cambrian apex predators

Giacinto De Vivo[1], Stephan Lautenschlager[2], Jakob Vinther[1]

[1]School of Earth Sciences and Biological Sciences, University of Bristol, 24 Tyndall Avenue, Bristol, BS8 1TQ, UK

[2]School of Geography, Earth and Environmental Sciences, University of Birmingham, B15 2TT, Birmingham, UK

Corresponding author:

ABSTRACT

Radiodonts evolved to become the largest nektonic predators in the Cambrian period persisting into the Ordovician and perhaps up until the Devonian period. They used a pair of large frontal appendages together with a radial mouth apparatus to capture and manipulate their prey and had evolved a range of species with distinct appendage morphologies already by the early Cambrian (~521 Ma). However, since their discovery, there has been a lack of understanding about their basic functional anatomy and thus their ecology. To explore radiodont modes of feeding we have digitally modelled different appendage morphologies represented by *Anomalocaris canadensis*, *Hurdia victoria*, *Peytoia nathorsti, Amplectobelua stephenensis*, and *Cambroraster falcatus* from the Burgess Shale. Our results corroborate ideas that there was likely a significant functional and, hence, behavioural diversity among different radiodont species with adaptations for feeding on differently sized prey (0.07 cm up to 10 cm). We argue here that *Cambroraster falcatus* appendages were suited for feeding on suspended particles rather than filtering sediment. Given the limited dexterity and lack of accessory feeding appendages as seen in modern arthropods, feeding must have been inefficient and ‘messy', which may explain their subsequent replacement by crown-group arthropods, cephalopods and jawed

vertebrates.

1. INTRODUCTION

Radiodonts were among the first large predators in metazoan dominated ecosystems that suddenly flourished near the onset of the Cambrian Series 2 (~ 521 Ma). Their fossil record extends to the Ordovician and potentially to the Lower Devonian (from ~419 to ~393 Ma) [1-11]. Members of this group exhibit a relatively large size, hydrodynamic body outline with elaborated natatory flaps, well-developed stalked compound eyes, and massive frontal raptorial appendages, which is evidence for them having been nektonic apex predators [2, 12-14].

Radiodonts are a clade of stem-euarthropods (Radiodonta) and comprise four main families (Amplectobeluidae, Anomalocaridae, Tamisiocaridae, and Hurdiidae) [11, 15-20]. Their frontal appendages comprise a series of hard elements (podomeres) intercalated by a soft and flexible region (arthrodial membrane). Two lateral articulating joints are placed between each podomere, dividing the arthrodial membrane into two parts, a ventral and dorsal [1, 2]. Each podomere may bear spines. In the past, researchers recognised two principal types of appendages among radiodonts: the Anomalocaridae-like appendages, showing a pair of endites, or ventral spines, projecting to form an inverted V-shape, and the Hurdiidae-like type (or F-type) appendages, bearing one single long endite [1]. Recent discoveries have revealed intermediate morphologies and other morphotypes of which the pincer-like frontal appendage of Amplectobeluidae is the most distinct [16, 20-22].

The diverse appendage morphologies among different radiodont species already established by the early stages of the Cambrian period is indicative of an adaptive radiation [16], reflecting diversification and partitioning into different feeding strategies, including filter-feeding. Filter-feeding has evolved many times throughout history amongst

53 nektonic top predators (tertiary/quaternary consumers) [11, 16, 23-26].

54 Adaptive radiations occur in the presence of new ecological opportunities [27].
55 Those may be offered by morphological innovation, colonising new ecospace or the
56 ecosystem vacuum post-dating a major extinction event [27]. The Cambrian was both a
57 time of innovation and ecological vacuums as a result of the emerging body plans.
58 Different animal phyla colonised the water column as predators to create the first
59 complexly tiered metazoan food web [28, 29]. Arthropods were dominant throughout most
60 of the Palaeozoic and occupied several tiers in the food chain up until jawed vertebrates
61 displaced the higher tiers in marine ecosystems [30]. Radiodonts pioneered this trend as
62 one of the first groups of nektonic predators with large body size and diverse feeding
63 structures.

64 Various hypotheses have been proposed to explain the functional roles radiodont
65 feeding structures may have served (frontal appendages and mouth apparatus), but none
66 have been tested. *Anomalocaris canadensis* is generally thought to have been a stealthy
67 macro predator [2, 13, 20, 21, 31] that grasped large prey, while the appendages of *Hurdia*
68 *victoria* and *Peytoia nathorsti* have been proposed to have worked as a jaw or sieve to
69 prior shift sediment [21, 32, 33]. The amplectobeluid appendage is posed to have
70 functioned as grasping/cutting pincers and *Cambroraster falcatus* has been interpreted as
71 sediment sifter [20, 21, 31-36], while the delicate accessory spines/bristles in members of
72 the tamisiocaridae and *Aegirocassis* and *Pahvantia* served in filter-feeding. Radiodonts
73 lack compelling modern analogues as they possess only a single pair of feeding
74 appendages. In contrast, extant arthropods typically possess a series of appendages with
75 specialised and differentiated elements for food manipulation. Furthermore, the radiodont
76 mouth apparatus otherwise found in other ecdysozoan phyla and the panarthropod total
77 group was lost.

78 Therefore, a new method is proposed, comprising the reconstruction of 3-D models

of radiodont appendages to explore their range of movement. We use this method to test and reconstruct differences in feeding and prey partitioning among the Burgess Shale radiodonts *Anomalocaris canadensis*, *Hurdia victoria*, *Peytoia nathorsti, Amplectobelua stephenensis* and *Cambroraster falcatus*. We have chosen the Burgess shale as a case study due to the diverse number of well-studied and illustrated taxa of which many likely co-existed. Understanding how radiodonts evolved to occupy a set of distinct trophic niches will improve our understanding of the complexity of Cambrian ecosystems and their role in shaping them [37-40].

2. MATERIAL AND METHODS

2.1 Museum abbreviations

The following prefixes are used: Royal Ontario Museum, Toronto (ROMIP); National Museum of Natural History, Washington (USNM); Mineralogisk Museum, Copenhagen (MMK); Geological Survey of Canada (GSC).

2.2 Species analysed

3-D models of the frontal appendage of *Anomalocaris canadensis*, *Amplectobelua stephenensis*, *Cambroraster falcatus, Hurdia victoria*, and *Peytoia nathorsti* (5 spine morphology) were constructed from measurements taken from the following specimens. *Anomalocaris canadensis*: ROMIP 51211, ROMIP 51212, ROMIP 51215, ROMIP 5124, ROMIP 62542, ROMIP 61040, ROMIP 61655, ROMIP 62543, USNM 57555, USNM 57490, USNM80487, GSC 45308, MMK 1925.87, USNM 213687; *Amplectobelua stephenensis*: ROMIP 59492, ROMIP 5493, ROMIP 59495; *Hurdia victoria*: ROMIP 60026, ROMIP 60048, ROMIP 60020, ROMIP 59259; *Cambroraster falcatus*: ROMIP 65084, ROMIP 65080, ROMIP 65085, ROMIP 65087; *Peytoia nathorsti*: USNM 240989. USNM 139709, USNM 57490, ROMIP 60052, ROMIP 60036, ROMIP 60044.

105

106 **2.3 Measurements**

107 The following measurements were taken of the appendage for each species using ImageJ
108 1.38e [41]: the dorsal and the ventral length, the proximal height, the length of the proximal
109 margin of the endite, the height of the articulating joint, the minimal and maximal length of
110 auxiliary spines, the maximal space between spines, and the diameter of the mouth (see
111 supplementary Figure 1). The ratio between the ventral and dorsal length, the dorsal
112 length and proximal height, the proximal height and the proximal margin of the endite
113 length, were also calculated for each podomere. Average values for each
114 measurement/ratio were also calculated to aid in the construction of models.

115

116 **2.4 Model creation and range-of-motion reconstruction**

117 A representative fossil specimen of a frontal appendage with proportions closest to
118 average values were selected and used to produce an interpretative drawing.

119 The interpretative drawing was then imported as a background image in Blender
120 2.81 (a professional open-source 3-D computer graphics software programme) and used
121 as a template to build the 3-D model through "box modelling" [42-44]. Podomeres and
122 endites were shaped by modifying (scaling, rotating, translating) in-built meshes (cube,
123 cones). Where necessary, the dimensions of the podomere elements were adjusted to the
124 average values taken in the previous step and other anatomical details, such as auxiliary
125 spines, were added.

126 Once completed, the model was articulated by a Blender armature using
127 interconnected elements (referred to as “bones”) to control the movement of the model.
128 Each bone of the armature was set as parent to the respective podomere and manually
129 moved into different configurations (e.g., fully extended, fully contracted) using forward
130 kinematics. The model was then compared to the positions shown in different fossils

preserved at an angle to estimate the lateral depth of the appendages following Briggs and Williams' observations for the reconstruction of flattened fossils [45], showing that a compression fossil is a 2-D representation of the specimen in 3-D. In other words, the lack of lateral distortion during compaction means that differently angled views allow for inferring the thickness of the fossil (see supplementary Information 1 a and b). Some species are not collected with sufficient variation in burial mode to expose different viewing angles other than lateral (as in *Amplectobelua stephenensis*) meaning that the appendage depth is poorly understood, including potential lateral curvature of spines.

The lateral articulation points between the appendage podomeres result in dorsoventral flexibility in a two-dimensional plane. The reconstructed range of movement was achieved by rotating the podomeres around the axis connecting the two articulating joints between adjacent podomeres, hence reducing the arthrodial membrane area until podomeres abut. By comparing fossils showing different grades of contraction and, in some cases, podomere overlap, we have also allowed some models to hyperextend/flex if deemed likely that the podomeres could allow for some degree of telescoping inferred when modelling the range of movement. The range of movement reported here should therefore be considered a minimum estimate of maximum extension/flection. It was not possible to infer a range of movement confidently in the most distal podomeres.

Once the model was articulated, an animated video and pictures of the model in different poses were rendered (see supplementary Video 1-5). From these, measurements of the contraction and extension angles were obtained between podomeres.

The position of the appendages relatively to the body in articulated specimens suggests a degree of movement beyond a two-dimensional plane in the junction between the limb and body. The membrane connecting the limb to the body is often termed the 'cormus'. A similar degree of dexterity is common among modern arthropods, where the cormus typically allows for the appendage to perform both dorsoventral and lateral

157 movements to different degrees [27, 46]. We, therefore, assume that radiodont
158 appendages had a higher degree of freedom of movement in the connection to the body.
159 This degree of freedom, however, remains to be fully assessed (see supplementary
160 Information 1 c).
161
162 **3. RESULTS**
163 Our findings indicate significant variation in the range of movements between the species
164 analysed (see supplementary Information, section 2 and supplementary Table 1 for more
165 details).
166 *Anomalocaris canadensis* (see Figure 1) possessed very dextrous appendages with a high
167 degree of flexibility (213°± 6° total and on average ~18° flection between podomeres) The
168 articulating joints are placed at ~80% of the proximal height of the podomere. In articulated
169 specimens, appendages are occasionally found with the ventral surface facing the other
170 appendage. This might indicate synchronised movements, although a single appendage
171 might have been sufficient to firmly grab prey (see supplementary Video 1) [31]. The
172 internal diameter of the space created by a minimally flexed appendage able to grab an
173 object is 20-28% of the total appendage dorsal length.
174 The appendages of *Peytoia nathorsti* (see Figure 2 a-d) are here inferred to have
175 exhibited less dexterity than *A. canadensis*, evidenced by the articulating joints placed
176 more medially, at ~70% of the podomere proximal height, offering a lower contractibility.
177 There is also a lower inferred extension angle (192°± 3° of total and on average ~22°
178 extension between podomeres). The proximal five podomeres show higher extension
179 angles (average ~27°) than the distal ones (average ~17°). Based on the range of
180 movement between each podomere and the mesial orientation of the auxiliary spines, a
181 single appendage might not have been sufficient to grab prey. The appendages might
182 have been used in concert, surrounding the prey while extended and capturing it during

contraction (see supplementary Video 2). These observations can also be extended to the seven-spined appendages of other *Laggania* species [21] and *Hurdia victoria* (see supplementary video 3).

In comparison to *P. nathorsti*, the frontal appendages of *Hurdia victoria* (see Figure 2 e-h) show a degree of extension that is considerably lower (106°± 3° in total and on average ~10° extension between podomers) and possessed only one spine-free distal podomere. The articulation joints are at ~70% of the distal height. The higher extension angle occurs between podomeres six and seven (~25°).

Amplectobelua stephenensis (see Figure 2 i-n) exhibit articulating joints at ~80% of the proximal height and a low degree of flection (40°± 4° in total and on average ~3° flection between podomers). This is compensated by their pincer-like shape, which makes these appendages suited for grasping prey of small size (see supplementary Video 4). Based on the distance between the elongated endites and the appendage body, the maximum prey diameter is estimated to be 30% of the total appendage length.

In macropredatory taxa, there is overall a strong correspondence between the estimated prey size and the oral come diameter.

Cambroraster falcatus appendages show articulating joints placed at ~85% of the proximal height and a degree of extension of ~7° between podomere two to three and 10° between podomere three to five could be allowed (see Figure 3 a-c). This degree of extension, together with the strong curvature of the endites, enabled the creation of a well-developed feeding basket surrounding the mouth (see Figure 3 d-f and supplementary Video 5).

4. DISCUSSION

4.1 Functional differences in radiodont appendages

4.1.1 Ecological niche partitioning in the Burgess Shale community

The Burgess Shale ecosystem included at least five roughly contemporaneous radiodonts [34]. *Anomalocaris*, *Peytoia* and *Hurdia* fossils are widely distributed in the Burgess Shale (e.g. the Mouth Stephen locality, Raymond Quarry and Tulip beds) [47], *Amplectobelua* was found at the Mount Stephen locality [21] and *Cambroraster* comes from the Marble Canyon Site [34], which hosts a diverse assemblage of radiodonts comprising 11% of the fauna and are yet to be documented [21, 34, 47]. Daley and Budd (2010) [21] argued that the coexistence of such a variety of radiodonts in the Burges Shale biota required niche partitioning and that the evolution of different appendage morphologies reflects different feeding strategies. The analyses conducted in this study support this claim (see Figure 4).

With the appendages of presumed adult *Anomalocaris canadensis* specimens ranging from 100-180 mm in length, our model infers average prey size to be 20-50 mm in diameter (Figure 4 a and b). Since the oral cone is inferred to have been unable to process hard food, prey could have been soft-bodied or lightly sclerotised [12]. Based on the position and dexterity of the appendages, a flexible and hydrodynamic body [13], *A. canadensis*'s prey may have been predominantly nektonic (e.g. vetulicolians, nectocaridids, or swimming arthropods) and occasionally benthic (such as benthic unmineralized arthropods) (see Figure 4 a and b). Coprolites have been described in China and Australia, mainly composed of the remains of non-mineralised organisms, such as waptiid arthropods or *Isoxys*, which exhibit dimensions compatible with *Anomalocaris* or *Amplectobelua* as the defecator [48, 49]. Some of these coprolites also contain the cuticles of trilobites as a minor component, indicating occasional predation on hard-shelled organisms [48, 49].

Several studies have hypothesised that *Peytoia nathorsti* formed a net-like structure with its appendages to trap food and could be used together with either as sieves or as

jaws to capture larger prey [1, 2, 21, 32]. The first hypothesis is unlikely due to the shape and position of the auxiliary spines, which are present only on the distal side, facing those of the opposite appendage, and are too small, irregularly spaced and sized to form an effective food trap. The second hypothesis is supported by the fact that spines with an alternating length are usually observed in extant arthropod appendages specialised in capturing large prey, such as those found on mantids or giant isopods [50, 51]. A similar pattern is present on the teeth and beaks of vertebrates [52, 53]. By using both the appendages in concert the captured prey of *P. nathorsti* the same length of the appendages (around 60-100 mm). The most distal, spine-free podomeres may have helped trap and manipulate prey. The feeding appendages were also closer to the body than in *Anomalocaris* [2]. Based on these observations along with the configuration of the appendages on the body, we infer *P. nathorsti* to have captured less agile and benthic prey, but of likely larger size than *A. canadensis* (see Figure 4 c and d). These interpretations are also consistent with the more rigid and presumably less hydrodynamic body compared to *A. canadensis*.

Similarly to those of *P. nathorsti*, *Hurdia victoria* the frontal appendages might have worked in conjunction. They are comparatively smaller (around 20-40 mm) and less dextrous. These characteristics indicate that they were probably better suited to capture small epibenthic mobile and sessile organisms such as trilobites, lobopodians, and perhaps endobenthic priapulids (see Figure 4 e and f). The frontal appendages of *H. victoria* show a degree of extension that is considerably smaller than in *P. nathorsti*, thereby diminishing the length of the extension, making them less suitable for capturing agile prey [17, 32]. This interpretation is consistent with the trunk anatomy *of H. victoria*, such as the presence of vertically displaced lateral flaps, which would likely prevent rapid swimming [17, 32].

A single *Amplectobelua stephenensis* appendage was able to grab prey with a

diameter of around 20 mm [21]. The smaller ventral spines along every other podomere distally to the hypertrophied spine might have been used to hold and retain prey by adding more friction. The multi-segmented nature of the appendage might suggest they were mechanically less stable than appendages with fewer segments, such as the common arthropod cheliped and hence unlikely to be used for crushing, slicing or cutting larger prey. In contrast, these appendages could be well suited to perform precise and well-controlled movements to firmly grasp and manipulate prey to the mouth or tearing off pieces from larges carcasses (see Figure 4 g and h).

4.1.2 *Cambroraster falcatus* may have been a filter feeder.

Filter-feeding is a particular feeding mode in which food particles in suspension are collected from the water column by passing through a specialised filtering structure. Filter-feeding can be active or passive. Whale sharks and mysticete whales are examples of a particular active filter-feeding mode in which the water is engulfed and forced to pass through filtering structures (e.g. baleen in cetaceans) when expelled [54]. Several teleost fishes and chondrichthyans utilise gill rakers [23, 34, 51, 55]. In arthropods, suspension-feeding involves specialised appendages with fine setae and spines. Among nektonic suspension feeders, several strategies exist, such as lunge feeding (like in rorqual mysticetes), skimming/ram-feeding (e.g. balaenid whales, paddlefish or basking sharks) or through more active pumping of water through the filter apparatus by suction currents in fishes or mechanical pumping of water (e.g. krill and mysids) [56]. Passive suspension-feeding also exists among arthropods in which filter appendages form a fan-like net that is held up against the water current (porcelain crab, atyopsid shrimps and barnacles) [57, 58]. Among radiodonts, *Tamisiocaris borealis* (early Cambrian, Sirius Passet) was described as a sweep net filter feeder [16], resembling mysids while the giant *Aegirocassis benmoulae* (early Ordovician, Fezouata) and smaller, but similar *Pahvantia hastata*

(middle Cambrian, Utah) shows adaptations for skim/ram feeding [11, 26].

General observations, which serve to identify fossil and recent filter feeders, show that the feeding structures consist of elongated and slender, equally spaced structures forming a net with a regular mesh size [11, 16]. Furthermore, the filter-feeding apparatus needs to create a closed compartment, so that water is forced through the filter apparatus and not around it.

Despite being previously described as sediment sifter [33, 34], our analysis suggests that *Cambroraster* were better suited for filter-feeding given their long auxiliary spines, which is not encountered amongst extant taxa processing sediment, which have shorter and more robust structures. Exemplified in feeding strategies amongst modern teleost fishes and their gill raker apparatus (Figure 3 g and h) [55], the suspension-feeding cichlid *Chaetobranchopsis australis* exhibits elongated, regularly spaced gill rakers (figure 3 g). In contrast, the cichlid *Satanoperca pappaterra*, which sifts sediment, possesses gill rakers that are shorter and wider (figure 3 h) [55, 59, 60]. Long and slender filter elements do not appear suitable for sediment manipulation as sifting more dense and viscous sediment necessitates a more robust apparatus.

Based on extant comparisons, *Cambroraster falcatus,* with its long and delicate spine apparatus, does not appear suited for sediment processing. The spines are facing anteriorly, which would cause much strain if ploughed into a substrate. While it is possible that sediment was brought into suspension by other means, such as the head shield, we argue that feeding must have been in suspension and by filtering rather than direct manipulation of sediment by the frontal appendages.

Corroborating the filter-feeding ecology, we observe that with the configuration of the frontal appendages anterior to the mouth and pointing in a ventral direction, the long ventral spines with the inwards curvature could form a feeding basket by the juxtaposition of the two appendages while extended (see Figure 3 d-f and supplementary video 5).

Using the observed relationship between filter mesh size and prey diameter [16, 34, 51], we estimate a minimum prey size of 0.7-2 mm. The head shield elements may have facilitated and enhanced the capability of filter-feeding by the off channelling water into and through the filter-feeding appendages. The horseshoe-shaped head shield, the reduced number of vertically displaced flaps and the dorsally positioned eyes indicate a nekto-benthic lifestyle [33, 34].

4.2 Prey size, the mouth apparatus and radiodont feeding efficacy.

The oral cone of radiodonts is homologous to that of deeper stem-arthropods, such as the gilled lobopodians and the introvert apparatus seen in other ecdysozoans [38]. Yet, it shows higher structural integrity as revealed by the coherent assembly of its elements into a unit often found in isolation after moulting or decay [35]; it is composed of a series of plates arranged in a circle with each plate displaying a series of denticle-like structures facing orally with bigger plates overlapping smaller ones slightly. An elastic non-sclerotised region was present between each oral plate [12]. The total number of plates, their distribution, and proportion are variable depending on the species and the taxonomic group (e.g., in *Anomalocaris* it is triradial and in hurdiids tetraradial) [12, 35]. Whether the mouth apparatus could exert any degree of biting force is unclear [2, 12, 48]. It has been proposed that the oral cone functioned as a suction apparatus, like how many fish consume and ingest prey [34, 61]. By everting the external plates, a partial vacuum would have formed that would pull the captured prey into the mouth, which would mean that the maximal diameter of prey to be ingested should be less than the outer diameter of the oral cone. Pharyngeal teeth observed in some taxa [12] may have been used in mastication food upon ingestion.

Unlike euarthropods, radiodonts lack specialised head appendages that would enable them to process and transport prey. Gnathobase-like structures recently described

339 from *Amplectobelua* from Chengjiang may likely have been utilised in food intake, but their
340 wider distribution in other taxa remains to be shown. While we surmise some processing
341 could have been possible in radiodonts it may have been limited compared to most living
342 arthropods [62].

343 As such the feeding mechanisms of radiodonts must have been relatively inefficient
344 in comparison to living arthropods. In predatory taxa, feeding consisted of prey capture,
345 transport to the mouth and then ingestion via suction and subsequent mastication
346 performed by the pharyngeal teeth and perhaps the outer tooth plates as well [12, 21, 34,
347 48]. The lack of specialised appendages to process the food prior to ingestion, a condition
348 often found in modern arthropod, and the poor masticatory efficiency of the oral cone
349 might have resulted in a lower energy intake. Therefore, the subsequent evolution of
350 predators better able to effectively slice and cut prey, for improved digestive rate, such as
351 jawed vertebrates, cephalopods and modern arthropod clades, might explain the turnover
352 and ultimate demise of the once successful radiodonts.

353

354 **5. CONCLUSIONS AND FURTHER RESEARCH**

355 Our results confirm previous hypotheses that little trophic overlap between different
356 radiodont species may have existed in the Burgess Shale biota*. Anomalocaris canadensis*
357 may have been a fast and agile predator with highly dextrous feeding appendages,
358 capable of catching pelagic prey. In contrast, the hurdiids *Peytoia nathorsti* and *Hurdia*
359 *victoria* appear more suited to capturing proportionally larger, but less agile prey and with a
360 near-benthic foraging strategy. The claw-like appendages of *Ambectobelua stephenensis,*
361 on the other hand, may have facilitated well-controlled grasping for catching smaller
362 animals (see Figure 4 i). *Cambroraster* is here interpreted as a suspension feeder as the
363 apparatus does not conform to sediment ingesting anatomy.

364 The inferred prey size of *Anomalocaris canadensis*, *Hurdia victoria*, and *Peytoia*

365 *nathorsti* is slightly inferior to the mouth diameters. This suggests prey was swallowed
366 whole and corroborates that the mouth mainly served for ingestion through the creation of
367 a suction current as observed in spiders and unlike most crown-euarthropods, which
368 process their prey by extensive mastication prior to ingestion or pre-digestion.
369
370 **6. ACKNOWLEDGEMENTS**
371 We are thankful to Imran Rahman for his help and technical advice. Jean-Bernard Caron,
372 Allison Daley, Stephen Pates generously shared high-resolution images. Our gratitude
373 goes also to Russell Garwood and two anonymous referees for their comments and
374 suggestions, which were crucial to improving the quality of the manuscript.
375
376 **Data accessibility**. The datasets supporting this article can be obtained from the
377 University of Bristol Data repository:
378 https://doi.org/10.5523/bris.1anaxh0xxbeg22o1gfsgl50ukh.

REFERENCES

1. Briggs D.E.G. 1979 *Anomalocaris*, the largest known Cambrian arthropod. *Paleontology* **22**, 631-664.
2. Whittington H.B., Briggs D.E.G. 1985 The largest Cambrian animal, *Anomalocaris*, Burgess Shale, British-Columbia. *Philosophical Transactions of the Royal Society of London B, Biological Sciences* **309**(1141), 569-609. (doi:10.1098/rstb.1985.0096).
3. Chen J.-y., Ramsköld L., Zhou G.-q. 1994 Evidence for monophyly and arthropod affinity of Cambrian giant predators. *Science* **264**(5163), 1304-1308. (doi:10.1126/science.264.5163.1304).
4. Montgomery D.R., Panfil M.S., Hayes S.K. 1999 Channel-bed mobility response to extreme sediment loading at Mount Pinatubo. *Geology* **27**(3), 271-274. (doi:10.1130/0091-7613(1999)027<0271:Cbmrte>2.3.Co;2).
5. Briggs D.E., Lieberman B.S., Hendricks J.R., Halgedahl S.L., Jarrard R.D. 2008 Middle Cambrian arthropods from Utah. *Journal of Paleontology* **82**(2), 238-254. (doi:10.1666/06-086.1).
6. Kühl G., Briggs D.E.G., Rust J. 2009 A great-appendage arthropod with a radial mouth from the Lower Devonian Hunsrück Slate, Germany. *Science* **323**(5915), 771-773. (doi:10.1126/science.1166586).
7. DALEY A.C., PEEL J.S. 2010 A possible anomalocaridid from the Cambrian Sirius Passet lagersätte, North Greenland. *Journal of Paleontology* **84**(2), 352-355. (doi:10.1666/09-136r1.1).
8. Ponomarenko A.G. 2010 First record of dinocarida from Russia. *Paleontological Journal* **44**(5), 503-504. (doi:10.1134/S0031030110050047).
9. Van Roy P., Briggs D.E.G. 2011 A giant Ordovician anomalocaridid. *Nature* **473**(7348), 510-513. (doi:10.1038/nature09920).
10. DALEY A.C., LEGG D.A. 2015 A morphological and taxonomic appraisal of the oldest anomalocaridid from the Lower Cambrian of Poland. *Geological Magazine* **152**(5), 949-955. (doi:10.1017/s0016756815000412).
11. Van Roy P., Daley A.C., Briggs D.E.G. 2015 Anomalocaridid trunk limb homology revealed by a giant filter-feeder with paired flaps. *Nature* **522**(7554), 77-80. (doi:10.1038/nature14256).
12. Daley A.C., Bergström J. 2012 The oral cone of *Anomalocaris* is not a classic ''peytoia''. *Naturwissenschaften* **99**(6), 501-504. (doi:10.1007/s00114-012-0910-8).
13. Usami Y. 2006 Theoretical study on the body form and swimming pattern of *Anomalocaris* based on hydrodynamic simulation. *Journal of Theoretical Biology* **238**(1), 11-17. (doi:https://doi.org/10.1016/j.jtbi.2005.05.008).
14. Paterson J.R., Edgecombe G.D., García-Bellido D.C. 2020 Disparate compound eyes of Cambrian radiodonts reveal their developmental growth mode and diverse visual ecology. *Science Advances* **6**(49), eabc6721. (doi:10.1126/sciadv.abc6721).
15. Collins D. 1996 The "evolution" of *Anomalocaris* and its classification in the arthropod class Dinocarida (nov.) and order Radiodonta (nov.). *Journal of Paleontology* **70**(2), 280-293. (doi:https://doi.org/10.1017/S0022336000023362).
16. Vinther J., Stein M., Longrich N.R., Harper D.A.T. 2014 A suspension-feeding anomalocarid from the Early Cambrian. *Nature* **507**(7493), 496-499. (doi:10.1038/nature13010).
17. Daley A.C., Budd G.E., Caron J.-B., Edgecombe G.D., Collins D. 2009 The Burgess Shale Anomalocaridid *Hurdia* and its significance for early Euarthropod evolution. *Science* **323**(5921), 1597-1600. (doi:10.1126/science.1169514).
18. Budd G.E., Telford M.J. 2009 The origin and evolution of arthropods. *Nature* **457**(7231), 812-817. (doi:10.1038/nature07890).
19. Cong P., Ma X., Hou X., Edgecombe G.D., Strausfeld N.J. 2014 Brain structure resolves the segmental affinity of anomalocaridid appendages. *Nature* **513**(7519), 538-542. (doi:10.1038/nature13486).

20. Pates S., Daley A.C. 2019 The Kinzers Formation (Pennsylvania, USA): the most diverse assemblage of Cambrian Stage 4 radiodonts. *Geological Magazine* **156**(7), 1233-1246. (doi:10.1017/S0016756818000547).
21. DALEY A.C., BUDD G.E. 2010 New anomalocaridid appendages from the Burgess Shale, Canada. *Palaeontology* **53**(4), 721-738. (doi:https://doi.org/10.1111/j.1475-4983.2010.00955.x).
22. Pates S., Daley A.C., Butterfield N.J. 2019 First report of paired ventral endites in a hurdiid radiodont. *Zoological Letters* **5**(1), 18. (doi:10.1186/s40851-019-0132-4).
23. Friedman M. 2012 Parallel evolutionary trajectories underlie the origin of giant suspension-feeding whales and bony fishes. *Proceedings of the Royal Society B: Biological Sciences* **279**(1730), 944-951. (doi:http://doi:10.1098/rspb.2011.1381).
24. Sims D.W., Southall E.J., Tarling G.A., Metcalfe J.D. 2005 Habitat-specific normal and reverse diel vertical migration in the plankton-feeding basking shark. *Journal of Animal Ecology*, 755-761. (doi:http://doi:10.1111/j.1365-2656.2005.00971.x).
25. Motani R., Chen X.-h., Jiang D.-y., Cheng L., Tintori A., Rieppel O. 2015 Lunge feeding in early marine reptiles and fast evolution of marine tetrapod feeding guilds. *Scientific Reports* **5**(1), 8900. (doi:10.1038/srep08900).
26. Lerosey-Aubril R., Pates S. 2018 New suspension-feeding radiodont suggests evolution of microplanktivory in Cambrian macronekton. *Nature Communications* **9**(1), 3774. (doi:10.1038/s41467-018-06229-7).
27. Garwood R., Dunlop J. 2014 The walking dead: Blender as a tool for paleontologists with a case study on extinct arachnids. *Journal of Paleontology* **88**(4), 735-746. (doi:10.1666/13-088).
28. Erwin D.H., Valentine J.W. 2013 *The cambrian explosion*.
29. Jonathan B. Losos. 2010 Adaptive radiation, ecological opportunity, and evolutionary determinism. *The American Naturalist* **175**(6), 623-639. (doi:10.1086/652433).
30. KLUG C., KRÖGER B., KIESSLING W., MULLINS G.L., SERVAIS T., FRÝDA J., KORN D., TURNER S. 2010 The Devonian nekton revolution. *Lethaia* **43**(4), 465-477. (doi:https://doi.org/10.1111/j.1502-3931.2009.00206.x).
31. Daley A.C., Edgecombe G.D. 2014 Morphology of *Anomalocaris canadensis* from the Burgess Shale. *Journal of Paleontology* **88**(1), 68-91. (doi:10.1666/13-067).
32. Daley A.C., Budd G.E., Caron J.-B. 2013 Morphology and systematics of the anomalocaridid arthropod Hurdia from the Middle Cambrian of British Columbia and Utah. *Journal of Systematic Palaeontology* **11**(7), 743-787. (doi:10.1080/14772019.2012.732723).
33. Liu Y., Lerosey-Aubril R., Audo D., Zhai D., Mai H., Ortega-Hernández J. 2020 Occurrence of the eudemersal radiodont *Cambroraster* in the early Cambrian Chengjiang Lagerstätte and the diversity of hurdiid ecomorphotypes. *Geological Magazine* **157**(7), 1200-1206. (doi:10.1017/S0016756820000187).
34. Moysiuk J., Caron J.-B. 2019 A new hurdiid radiodont from the Burgess Shale evinces the exploitation of Cambrian infaunal food sources. *Proceedings of the Royal Society B: Biological Sciences* **286**(1908), 20191079. (doi:doi:10.1098/rspb.2019.1079).
35. Liu J., Lerosey-Aubril R., Steiner M., Dunlop J.A., Shu D., Paterson J.R. 2018 Origin of raptorial feeding in juvenile euarthropods revealed by a Cambrian radiodontan. *National Science Review* **5**(6), 863-869. (doi:10.1093/nsr/nwy057).
36. Guo J., Pates S., Cong P., Daley A.C., Edgecombe G.D., Chen T., Hou X. 2019 A new radiodont (stem Euarthropoda) frontal appendage with a mosaic of characters from the Cambrian (Series 2 Stage 3) Chengjiang biota. *Papers in Palaeontology* **5**(1), 99-110. (doi:https://doi.org/10.1002/spp2.1231).
37. Vannier J., Liu J., Lerosey-Aubril R., Vinther J., Daley A.C. 2014 Sophisticated digestive systems in early arthropods. *Nature Communications* **5**(1), 3641. (doi:10.1038/ncomms4641).

38. Vinther J., Porras L., Young F.J., Budd G.E., Edgecombe G.D. 2016 The mouth apparatus of the Cambrian gilled lobopodian *Pambdelurion whittingtoni*. *Palaeontology* **59**(6), 841-849. (doi:https://doi.org/10.1111/pala.12256).
39. Whittington H.B. 1975 The enigmatic animal *Opabinia regalis*, middle Cambrian, Burgess Shale, British Columbia. *Philosophical Transactions of the Royal Society of London B, Biological Sciences* **271**(910), 1-43. (doi:doi:10.1098/rstb.1975.0033).
40. Budd G.E. 1998 The morphology and phylogenetic significance of *Kerygmachela kierkegaardi* Budd (Buen Formation, Lower Cambrian, N Greenland). *Earth and Environmental Science Transactions of The Royal Society of Edinburgh* **89**(4), 249-290. (doi:https://doi.org/10.1017/S0263593300002418).
41. Sheffield J.B. 2007 ImageJ, a useful tool for biological image processing and analysis. *Microscopy and Microanalysis* **13**(S02), 200-201. (doi:https://doi.org/10.1017/S1431927607076611).
42. Hess R. 2007 *The Essential Blender: guide to 3D creation with the open source suite Blender*, No Starch Press.
43. Rahman I., Lautenschlager S. 2017 Applications of three-dimensional box modeling to paleontological functional analysis. *Paleontological Society Papers* **22**, 119-132.
44. Lautenschlager S. 2015 Estimating cranial musculoskeletal constraints in theropod dinosaurs. *Royal Society Open Science* **2**(11), 150495. (doi:doi:10.1098/rsos.150495).
45. BRIGGS D.E.G., WILLIAMS S.H. 1981 The restoration of flattened fossils. *Lethaia* **14**(2), 157-164. (doi:https://doi.org/10.1111/j.1502-3931.1981.tb01918.x).
46. Hou X.J., Bergstrom. 1997 *Arthropods of the Lower Cambrian Chengjiang fauna, southest China*, Scandinavian University press.
47. Nanglu K., Caron J.-B., Gaines R.R. 2020 The Burgess Shale paleocommunity with new insights from Marble Canyon, British Columbia. *Paleobiology* **46**(1), 58-81. (doi:10.1017/pab.2019.42).
48. Nedin C. 1999 *Anomalocaris* predation on nonmineralized and mineralized trilobites. *Geology* **27**(11), 987-990. (doi:10.1130/0091-7613(1999)027<0987:Aponam>2.3.Co;2).
49. VANNIER J., CHEN J. 2005 Early cambrian food chain: new evidence from fossil aggregates in the Maotianshan Shale Biota, SW China. *PALAIOS* **20**(1), 3-26. (doi:10.2110/palo.2003.p03-40).
50. Van Roy P., Tetlie O.E. 2006 A spinose appendage fragment of a problematic arthropod from the Early Ordovician of Morocco. *Acta Palaeontologica Polonica* **51**(2), 239-246.
51. Brannoch S.K., Wieland F., Rivera J., Klass K.-D., Béthoux O., Svenson G.J. 2017 Manual of praying mantis morphology, nomenclature, and practices (Insecta, Mantodea). *ZooKeys* **696**. (doi:10.3897/zookeys.696.12542).
52. WAINWRIGHT P.C., BELLWOOD D.R., WESTNEAT M.W., GRUBICH J.R., HOEY A.S. 2004 A functional morphospace for the skull of labrid fishes: patterns of diversity in a complex biomechanical system. *Biological Journal of the Linnean Society* **82**(1), 1-25. (doi:10.1111/j.1095-8312.2004.00313.x).
53. Louchart A., Sire J.-Y., Mourer-Chauviré C., Geraads D., Viriot L., de Buffrénil V. 2013 Structure and growth pattern of Pseudoteeth in *Pelagornis mauretanicus* (Aves, Odontopterygiformes, Pelagornithidae). *PLOS ONE* **8**(11), e80372. (doi:10.1371/journal.pone.0080372).
54. Croll D.A., Tershy B.R., Newton K.M., de Vos A., Hazen E., Goldbogen J.A. 2018 Filter Feeding. In *Encyclopedia of Marine Mammals (Third Edition)* (eds. Würsig B., Thewissen J.G.M., Kovacs K.M.), pp. 363-368, Academic Press.
55. Collard F., Gilbert B., Eppe G., Roos L., Compère P., Das K., Parmentier E. 2017 Morphology of the filtration apparatus of three planktivorous fishes and relation with ingested anthropogenic

524 particles. *Marine Pollution Bulletin* **116**(1), 182-191.
525 (doi:https://doi.org/10.1016/j.marpolbul.2016.12.067).
526 56. Anderson D.T. 1981 Cirral activity and feeding in the barnacle *Balanus perforatus* Bruguiére
527 (Balanidae), with comments on the evolution of feeding mechanisms in thoracican cirripedes.
528 *Philosophical Transactions of the Royal Society of London B, Biological Sciences* **291**(1053), 411-
529 449. (doi:doi:10.1098/rstb.1981.0004).
530 57. Gabaldon D.J. 1979 Observation of a possible alternate mode of feeding in a porcellanid
531 crab (Petrolisthes Cabrilloi Glassell, 1945) (Decapoda, Anomura). *Crustaceana* **36**(1), 110-112.
532 (doi:https://doi.org/10.1163/156854079X00285).
533 58. Hamner W.M. 1988 Biomechanics of filter feeding in the antarctic krill *Euphausia Superba*:
534 Review of Past Work and New Observations. *Journal of Crustacean Biology* **8**(2), 149-163.
535 (doi:10.2307/1548308).
536 59. Khalaf-Allah H., Azab A., Mohamed A. 2016 Morphological differences of gill rakers in some
537 sparid fish species (Family: Sparidae), Egypt. *International journal of environmental science and*
538 *engineering (IJESE)* **7**, 63-72.
539 60. Novakowski G.C., Cassemiro F.A.S., Hahn N.S. 2016 Diet and ecomorphological
540 relationships of four cichlid species from the Cuiabá River basin. *Neotropical Ichthyology* **14**.
541 61. Gibb A.C., Ferry-Graham L. 2005 Cranial movements during suction feeding in teleost
542 fishes: Are they modified to enhance suction production? *Zoology* **108**(2), 141-153.
543 (doi:https://doi.org/10.1016/j.zool.2005.03.004).
544 62. Cong P., Daley A.C., Edgecombe G.D., Hou X. 2017 The functional head of the Cambrian
545 radiodontan (stem-group Euarthropoda) *Amplectobelua symbrachiata*. *BMC Evolutionary Biology*
546 **17**(1), 208. (doi:10.1186/s12862-017-1049-1).
547

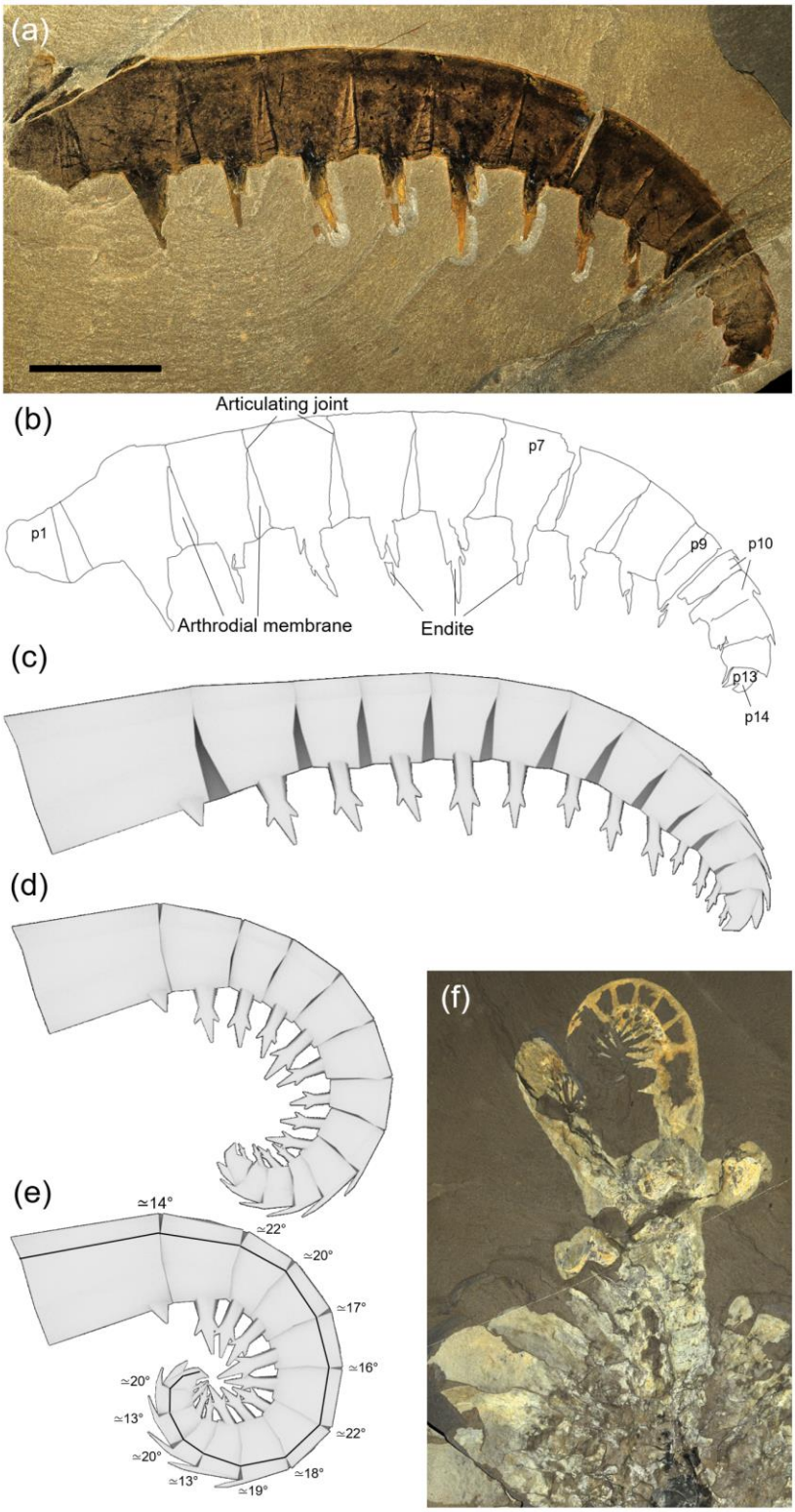

Figure 1 Frontal appendage of *Anomalocaris canadensis* (*a*) specimen ROMIP 61040), (*b*) interpretative drawing and the (*c*) reconstructed appendage model; comparison between the model showing the degree of flection (*d*) based on the sole arthrodial membrane and (*e*) on the contact between the ventral spines as shown in (*f*) the specimen ROMIP 51212 (f). The bars in (e) indicate the bones of the Blender armature with their relative articulation joints and the computed angles of flection between each podomere. Scale bar 20 mm.

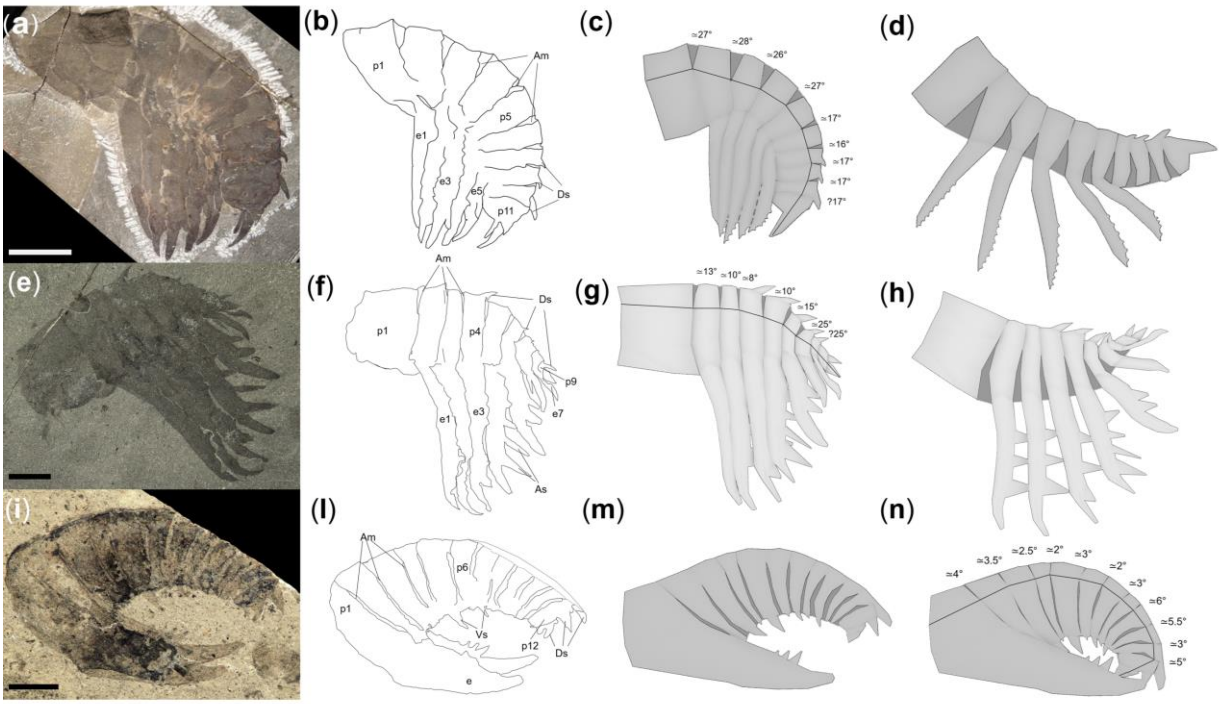

Figure 2 Radiodont frontal appendage reconstructions. (a-d) *Peytoia nathorsti* (*a*) specimen USNM 240984, (*b*) interpretative drawing and (*c*) the flexed and (*d*) extended model of the appendage; (e-h) *Hurdia victoria*, (*e*) specimen ROMIP 59259, (*f*) interpretative drawing and (*g*) the flexed and (*h*) extended model of the appendage; (i-m) *Amplectobelua stephenensis*, (*i*) specimen ROMIP 59495, (*j*) interpretative drawing and (l) the flexed and (m) extended model of the appendage. Scale bars in (a) 10 mm, in (e) and (i) 5 mm. The bars in (*c*, *g*, n) indicate the bones of the Blender armature with their relative articulation joints and the computed angles of extension (*c*, *g*) or flection (n*)* between each podomere. Am = arthrodial membrane, As = auxiliary spine, Ds = dorsal spine, E = endite, P=podomere, Vs = ventral spines. Picture in (a) from [22].

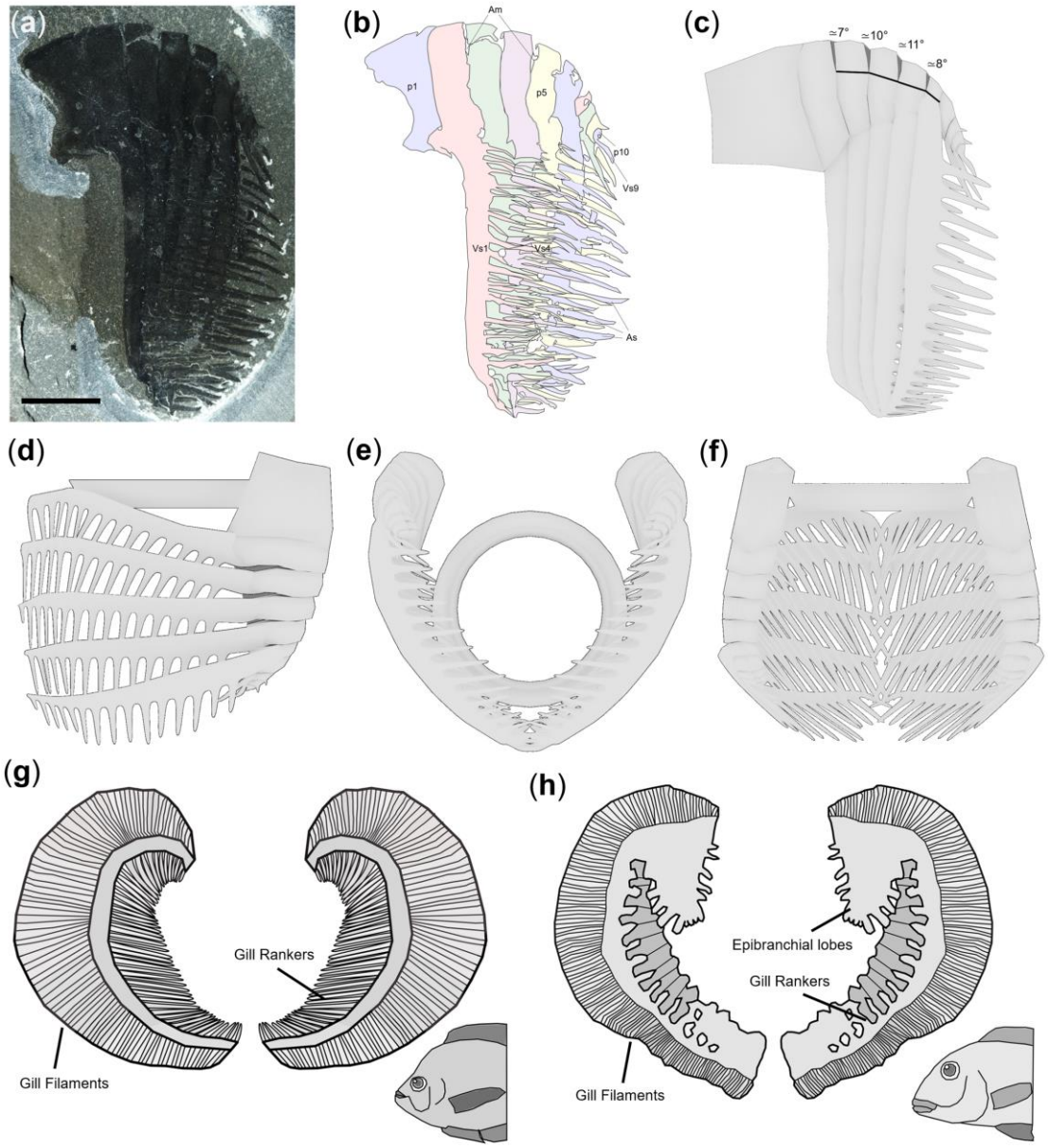

562

563 **Figure 3** Reconstruction of *Cambroraster falcatus* (*a*) specimen ROMIP 605084, (*b*) interpretative drawing and (*c*) the
564 reconstructed model of the appendage; Extended model forming a feeding basket in (*d*) lateral (, (*e*) ventral and (*f*) frontal
565 view surrounding the mouth apparatus (represented by the toroid). Comparison between the gill rankers of (*g*) the filter feeder
566 cichlid *Chaetobranchopsis australis* and the (*h*) deposit feeder *Satanoperca pappaterra* with the first being more elongated
567 and presenting interstitial space, similarly to the auxiliary spines of *Cambroraster falcatus*. Scale bar 10 mm. The bars in (*c*)
568 indicate the bones of the Blender armature with their relative articulation joints and the computed angles of extension (*c*)
569 between each podomere. Am = arthrodial membrane, As = auxiliary spine, Ds = dorsal spine, Vs = ventral spine. Images in
570 (*g*) and (*h*) modified from [50].

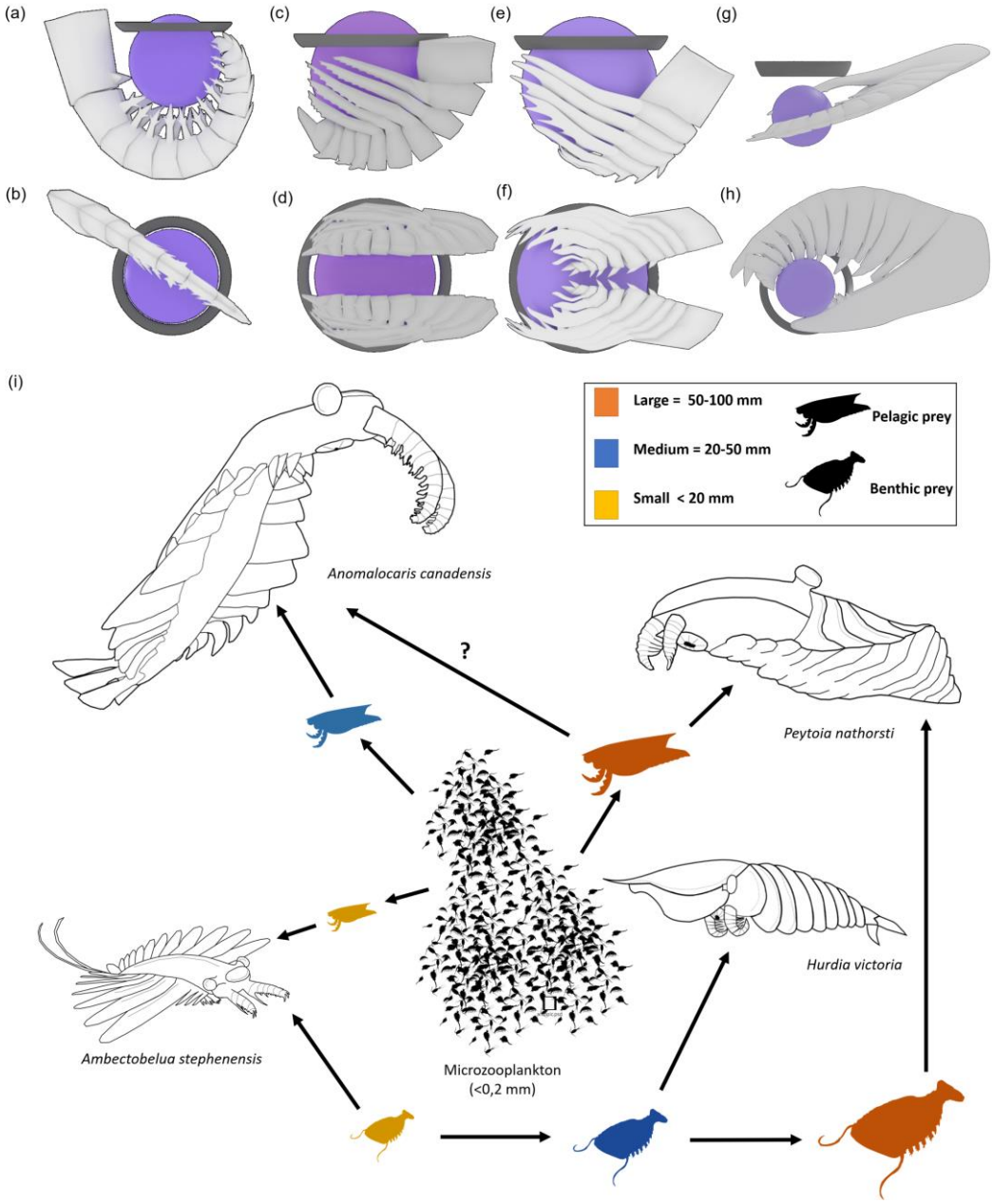

Figure 4 Reconstruction of radiodont feeding modes and inferred maximum prey size (represented by the violet sphere) compared to the mouth apparatus (represented by the dark grey toroid). *Anomalocaris canadensis* capturing its prey using a single appendage in (*a*) lateral and (*b*) dorsal view; *Peythoia nathorsti* capturing its prey using both appendages in conjunction, in (c) lateral and (d) dorsal view; *Hurdia victoria* capturing its prey using both appendages in conjunction, in (e) lateral and (f) dorsal view; *Amplectobelua stephenensis* capturing its prey using a single appendage, in (g) lateral and (h) dorsal view; (*i*) Niche partitioning among different Burges Shale radiodont species, arrows indicate the energy flow through the food chain. *Anomalocaris canadensis* was able to catch medium-size, or maybe larger, agile pelagic prey, whereas hurdiids such as *Hurdia victoria* and *Peytoia nathorsti* were more specialised to feed on benthic prey. *Peytoia* may have consumed pelagic prey also. Smaller benthic animals and the medium members of the nekton were captured by *Ambectobelua stephenensis*. Silhouettes from @Phylopic (Joanna Wolfe) and modified from illustrations made by Marianne Collins and Jun (https://twpf.jp/ni075).

SUPPLEMENTARY INFORMATION

3-D modelling, disparity, and ecology of the first Cambrian apex predators

Giacinto De Vivo[1], Stephan Lautenschlager[2], Jakob Vinther[1]

[1]School of Earth Sciences and Biological Sciences, University of Bristol, 24 Tyndall Avenue, Bristol, BS8 1TQ, UK

[2]School of Geography, Earth and Environmental Sciences, University of Birmingham, B15 2TT, Birmingham, UK

Table of contents

1- Examples of radiodont appendage reconstruction

a) Detailed example of a radiodont appendage reconstruction: *Anomalocaris canadensis.*

Measurements from a range of appendages attributed to *Anomalocaris canadensis* was taken from each podomere (Pdors, Plat, Pvent, SI, Supplementary Figure 1 A). From these, for each specimen, the ratio between different podomere elements was computed, as well the average ratios per the corresponding podomere between each specimen. Once this step was completed, we selected a representative and well preserved specimen as a template for the reconstruction (ROMIP 61040, Figure 1 A, main text). This specimen has average dimensions and shows clear podomere margins, arthrodial membranes, articulating joints. This specimen also consists of a well preserved part and counterpart. A detailed interpretative drawing was made (Figure 1 B, main text). The interpretative drawing was imported into Blender 2.81, and, using box modelling—a 2-dimensional model of the appendage was created. Each podomere and endite was shaped independently. Where the podomere was incompletely exposed or preserved, we used average proportions from our measurements from other specimens. For example, podomere 9 Pdors and Pvent have been computed knowing PI and the average proportions (Pdors/PI, Pvent/Pdors, Supplementary figure 1). Podomere 1 has been reconstructed using the Pdors ratio between its distal in the complete specimen (ROMIP 62543) and according to average ratios. We subsequently extruded the planar model to get a 3-D shape, to the depth revealed by specimens exposed in dorsoventral view. Because *Anomalocaris canadensis* appendages show an overall bilateral symmetry. We shaped half podomere and mirrored the other part. The width of the appendage was computed using the ratio between the Width and Pdors in ROM 616770 (Figure 12-8) [31]. ROMIP 616770 also shows a central “crest”, indicating a restriction of the dorsal margin. A central restriction in the ventral margin is indicated by the V-displacement of the pair endites shown in many specimens (e.g., ROMIP 62543, but also ROMIP 61040) (Figure 14-4) [31]. We modified the model accordingly giving the podomeres a quasi-elliptical shape.

b) Detailed example of a radiodont appendage reconstruction: The shape and the position of the endites in *Hurdia victoria.*

The model of *Hurdia victoria* was created using a similar procedure as reported for *A. canadensis* above. Differences in modelling lie in the reconstruction of the single long endites. Endites in *Hurdia* overlap: the proximal margin of one endite covers part of the distal endite in lateral view and the other way around in mesial view. Lateral and mesial view can be distinguished by the auxiliary spines being superimposed onto the overlapping endites. The shape of the proximal endites in *Hurdia* was modelled based on partially extended specimens like ROMIP 60048 (Figure 12-C) and ROMIP 60020 (Figure 12-E [32]. Once the planar shape of the endites was complete, we used a schematic drawing of the specimen ROMIP 65094 (Figure 3-G) [34] for reconstructing the orientation and the curvature of the endites (using the curve modifier on Blender 2.8) and the orientation of the spines. This specimen shows a *Hurdia* appendage in an almost frontal view, allowing for inferring their lateral arching trajectory. The insertion of endites is, as indicated by ROMIP 65095, laterally displaced.

c) The orientation and the movement at the cormus.

Based on articulated specimens, clues about the orientation and the position of the appendage relative to the mouth provide evidence for how dextrous the connecting membrane between the appendage and the

637 body (cormus) may have been in life: the appendages of *Anomalocaris canadensis* are typically oriented
638 frontally (see ROMIP 51212, figure 1 F, main text) while those of the hurdiids have a ventral orientation
639 relative to the body (e.g. USNM274142, figure 35 [2]; ROMIP 60012, figure 21-C [32]; ROMIP 65087, Figure
640 2-J [34]). Articulated specimens of *Amplectobelua stephenensis* have not been described yet.

641 Amongst extant arthropods, several muscle groups inserting into the first podomere from the body and
642 extensive articulating membranes facilitate a greater range of movements than the typical 2-dimensional
643 range between more distal podomeres. This was likely also the case in radiodonts.

644 It has been suggested that the shape of the distal margin of the peduncle should reveal the dexterity of the
645 appendage at the cormus [31]. This shape seems to be straight in *Anomalocaris canadensis* (ROM 51215,
646 Figure 10-1) [31] and convex in *Peytoia*, *Hurdia* and *Amplectobelua* (ROMIP 60052, Figure 13-A [32], ROMIP
647 59633; Figure 24-A [32]; ROM 59496, Figure 4-A [21]) which may provide some constraints as to what
648 directions of movements may have been permitted. While these must have offered some constraints as to
649 the range of movements, caution is advised. The notch shown in *Cambroraster* specimen ROMIP 605084
650 might be an artefact due to incomplete preservation. Its first podomere might have been longer, as shown
651 in ROMIP 65087 [31]. In many radiodont specimens, the first podomere is incomplete in its proximal part
652 and this might suggest a lower level of sclerotisation, that may have gone into facilitating a greater range of
653 movements [1]. It is also observed that in *A. canadensis*, the appendages are oriented at different angles in
654 body fossil specimens (ROMIP 51211, ROMIP 51212, and ROMIP 51213) [29], although post mortem
655 displacement and decay could result in unnatural postures. However, based on modern evidence and with
656 fossil evidence we consider radiodont frontal appendages to have had a higher range of movements at the
657 cormus, beyond a 2-dimensional plane. In our reconstructed range of movements, we have been aiming at
658 inferring a range of movements that are conservative and consistent with the evidence offered by the fossil
659 record.

2- Appendage morphology and range of movements

a) *Anomalocaris canadensis*

The available appendages of *Anomalocaris canadensis* vary from 30 to 180 mm in length and exhibit 14 podomeres with the 13 most proximal bearing a pair of tricuspid endites (see Figure 1 a and b). The overall length of the endites decreases distally, and longer and shorter spines alternate with the shortest spines located on uneven segments [1, 2, 31]. The articulation joints on both sides are almost ~80% of the proximal podomere height (specimens ROMIP 61040, ROMIP 62543) (see Figure 1 c).
The degree of flection indicated by the margins of the arthrodial membranes, ~11° on average and ~134° in total, (see Figure 2 d) do not permit the flexure observed in some specimens (see Figure 2 e-f). This limit might be indicated by the contact between endites rather than podomeres. From this, we estimate a degree of ventral telescoping close to 20% of the ventral length on each podomere.
Due to the lack of an expanded dorsal margin of the arthrodial membranes, the presence of dorsal spines on the most distal podomeres, and the fact that no specimen seems to show a higher degree of extension, we assume that the specimen ROMIP 61040 might be a fully extended appendage. Thus, from a wholly extended appendage, an average flection of ~18° between each podomere and a total flection of ~213° can be reconstructed (see Figure 2 e).
The internal diameter of the space created by a minimally flexed appendage able to grab an object is 20-28% of the total appendage dorsal length, a ratio akin to that measured between the oral cone diameter and the appendage length in ROMIP 51213, ROMIP 51215, ROMIP 61663, and ROMIP 61642 (25%).

b) *Peytoia nathorsti*

The described appendages in *Peytoia nathorsti* vary between 60 and 120 mm in length and are composed of eleven podomeres, of which only two to six bear endites [1, 2, 32]. Appendages are usually fully flexed. In some cases, such as in USNM 240984, it is possible to see the dorsal part of the arthrodial membrane and the position of the articulating joints (see Figure 2 a and b). The observed angle is on average ~22° between each podomere, with the proximal five podomeres showing a higher angle (average ~27°) than the distal one (average ~17°). The articulating joints comprise ~70% of the total proximal height (see Figure 2 c and d). A fully extended *Peytoia* appendage has not been described, although the most distal podomeres in specimen USNM 57490 display the ventral arthrodial membrane, which indicate a specific grade of extension [1, 22]. We interpret the flexed state to be the default, or relaxed, state, and that the appendage is extended during prey capture only.
Frontal appendages of *P. nathorsti* are found in paired constellations with the endites facing each other (specimen USNM 57490, USNM 139724), which might suggest that the appendages might have been used in concert to capture prey [1]. Auxiliary spines are different in lengths (between 0.6 to 1.8 mm) and do not exhibit regular spacing (between 0.3 to 1 mm in specimen USNM 240984, USNM 57490). USNM 57490 also demonstrates that the most distal podomeres curve medially slightly. Complete *Peytoia* appendages associated with the oral cone are not currently described and available for this study. The length of the isolated oral cone was similar to the total length of the appendages (USNM 57555) [2].

c) *Hurdia victoria*

Appendages in *Hurdia victoria* are usually not longer than 30 mm and shows 9 podomeres, from which, 8 (from 2 to 9) possess well-developed endite. Like other members of Hurdiidae, the endites are distally

pointing inward and slightly curved, and a triangular shape is visible in their transverse section [17, 32]. Endites 1 to 6 possesses auxiliary spines, while the eighth and the ninth podomeres host a well-developed non-spinous endite, 25% shorter than the others (see Figure 2 e and f). Like *Anomalocaris canadensis*, some body fossils exhibit configurations suggesting a degree of freedom of movement at the peduncular base (ROM 60035, ROM 59633) [17, 32]. The articulation joints are ~70% of the proximal height. Despite the fact that most hurdiid frontal appendages are found in a flexed condition, as observed in *P. nathorsti*, the dorsal articulating membrane is generally not evident; however, it can be observed in ROM 60048 and ROM 59259 (see Figure 2 e and f). Our analysis indicates an average of ~10° extension in between each of the first five podomeres. This value increases to ~25° between podomeres 6-7 (see Figure 2 g and h). The spacing between auxiliary spines ranged from 1-2 mm and each spine is up to 3 mm long within a single specimen (ROMIP 59259). The diameter of the mouth apparatus is equivalent to the total length of the appendages (ROM 60012, ROM 60035, ROM 59633) [17, 32].

d) *Amplectobelua stephenensis*

The two single appendages described are ~40 mm long and composed of twelve podomeres of which the first bear well-developed endites [21]. A single pair of smaller endites (less than 2 mm long) is present on uneven podomeres, and a pair of smaller ones on even podomeres. Podomere 2 and podomeres from 10 to 12 do not bear spines. Three auxiliary spines are present on the endites. The arthrodial membranes are present in ROM 59495 from which the articulating joint is estimated at ~80% of the proximal height. ROM 59495 also represent an almost fully extended appendage with the uneven podomeres endites spines at approximately the mid-length of their ventral margin (see Figure 2 i and l). From this specimen, a model has been produced and the degree of flection between each podomere seems not to be higher than ~6°, with an average of ~3°. Given the wider arthrodial membrane on the most distal podomeres, it might be possible that the tip of the appendage had some degree of extension, this cannot be assessed due to the incompleteness of the specimen. The space between the podomeres and the endite in a fully extended *Amplectobelua stephenensis* appendage offers a range indicating a capability of grasping prey smaller than 30% of the total length of the appendage.

e) *Cambroraster falcatus*

Cambroraster falcatus appendages are around 30 mm long and composed of ten podomeres. Except for the first and the seventh podomere, each podomere bears a single endite. Endites on podomeres 2 to 6 curve internally and, (almost two times the proximal height) and bear a series of long auxiliary spines (up to 8 mm) regularly spaced (up to 1,3 mm between each spine); the endites 8 and 9 are considerably shorter, spiniform and straight [34]. The specimen ROMIP 65084, on which the model was largely based, shows the dorsal part of the arthrodial membranes. Therefore, the articulating joint was placed at 85% of the proximal height and a degree of extension of ~7° between podomere two to three and 10° between podomere three to five could be allowed (see Figure 4 a-c). This degree of extension, together with the strong curvature of the endites, enabled the creation of a well-developed feeding basket surrounding the mouth (see Figure 4 d-f). This configuration can be partially observed in specimen ROMIP 65087, in which the appendages are partially extended, and the mouth apparatus is shown in relationship to the appendages, indicating roughly a similar size [34].

3- Supplementary Table 1

A. canadensis	**p1-p2**	**p2-p3**	**p3-p4**	**p4-p5**	**p5-p6**	**p6-p7**	**p7-p8**	**p8-p9**	**p9-p10**	**p10-p11**	**p11-p12**	**p12-p13**	**p13-p14**
Max. extension	174	178	177	171	169	164	168	169	159	159	154	146	165
Max. contraction	160	156	157	153	153	142	150	150	147	141	142	126	?
P. nathorsti	**p1-p2**	**p2-p3**	**p3-p4**	**p4-p5**	**p5-p6**	**p6-p7**	**p7-p8**	**p8-p9**	**p9-p10**	**p10-p11**			
Max. extension	182	193	188	182	188	180	187	194	172	?			
Max. contraction	155	165	163	154	172	163	170	177	155	156			
H. victoria	**p1-p2**	**p2-p3**	**p3-p4**	**p4-p5**	**p5-p6**	**p6-p7**	**p7-p8**	**p8-p9**					
Max. extension	187	189	182	186	173	200	194	?					
Max. contraction	174	179	173	176	158	175	171	137					
A. stephenensis	**p1-p2**	**p2-p3**	**p3-p4**	**p4-p5**	**p5-p6**	**p6-p7**	**p7-p8**	**p8-p9**	**p9-p10**	**p10-p11**	**p11-p12**		
Max. extension	180	179	172	171	172	171	175	172	173	154	138		
Max contraction	176	175	170	169	169	169	172	166	168	151	134		
C. falcatus	**p1-p2**	**p2-p3**	**p3-p4**	**p4-p5**	**p5-p6**	**p6-p7**	**p7-p8**	**p8-p9**	**p9-p10**				
Max. extension	169	175	180	171	168	?	?	?	?				
Max. contraction	169	168	169	160	160	165	170	168	163				

Supplementary Table 1 Maximal extension and contraction between the podomers and their distal ones among different radiodont species. Measures were taken between Pdors and reported in degrees.

4- List of supplementary material

Measurements.xlsx An Excel file containing all the measurements taken from the fossils.

Supplementaryvideo folder containing the following files:

- **Supplementaryvideo1.mkv** supplementary video of *Anomalocaris canadensis;*
- **Supplementaryvideo2.mkv** supplementary video of *Peytoia nathorsti;*
- **Supplementaryvideo3.mkv** supplementary video of *Hurdia victoria;*
- **Supplementaryvideo4.mkv** supplementary video of *Amplectobelua stephenensis;*
- **Supplementaryvideo5.mkv** supplementary video of *Cambroraster falcatus.*

Models folder containing the following files:

- **Acanadensis.blend** model of a single *A. canadensis* appendage;
- **AcanadensisAnim.blend** model of the *A. canadensis* appendages from which the video was rendered;
- **Amplectobelua.blend** model of a single *A. stephenensis* appendage;
- **AmplectobeluaAnim.blend** model of the *A. stephenensis* appendages from which the video was rendered;
- **Cambrotaster.blend** model of a single *A. stephenensis* appendage;
- **CambrorasterAnim.blend** model of the *C. falcatus* appendages from which the video was rendered;
- **Hurdia.blend** model of a single *H. victoria* appendage;
- **HurdiaAnim.blend** model of the *H. victoria* appendages from which the video was rendered;
- **Peytoia.blend** model of a single *P. nathorsti* appendage;
- **PeytoiaAnim.blend** model of the *P. nathorsti* appendages from which the video was rendered.

778

779 **5- List of the specimen cited in the manuscript.**

780 - ***Anomalocaris canadensis*:** ROMIP 51211 (Figure 2), ROMIP 51212 (Figure 1), ROMIP 51213 (Figure
781 8), ROMIP 1525 (Figure 10-1), ROMIP 62543, (Figure 13-5), ROMIP 61663 (Figure 11-1), ROMIP
782 61642 (Figure 12-1) [31].
783 - ***Peytoia nathorsti*:** USNM 57490, (Page 80, Figure 2), USNM 139724 (Page 80, Figure 8) [1], USNM
784 57538 (Figure 61) [2].
785 - ***Hurdia victoria*:** ROMIP 60035 (Figure 22-D), ROMIP 59633 (Figure 24-A), ROMIP 60048 (Figure 12-
786 D), ROMIP 60012 (Figure 21-D) [23].
787 - ***Cambroraster falcatus*:** ROMIP 65080 (Figure 2-C) ROMIP 65087 (Figure 2-J) [34].

6- Supplementary Figure 1

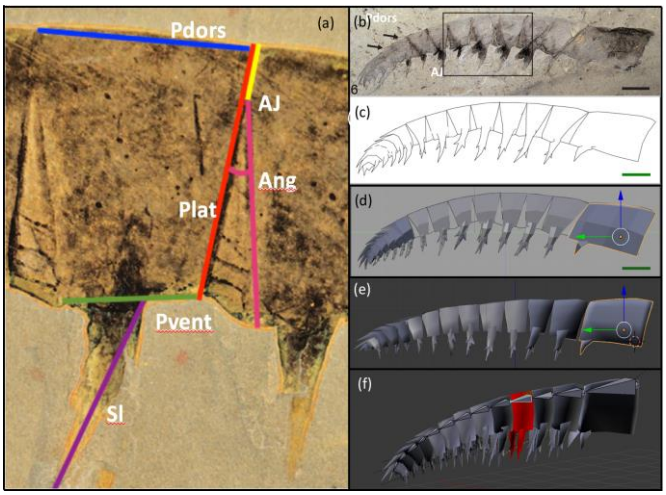

Supplementary Figure 1. Process used in this study at different stages for appendage reconstruction exemplified by *Anomalocaris canadensis*: measurements taken and their abbreviated labelling (a), Fossil chosen to build model upon (b) and its interpretative sketch (c), 3-D model using box modelling (d), correction using the average measures (e), blender armature application to a single appendage (f). Aj= the articulating joint, Ang= articulating joint angle, Pdors= dorsal length, Pvent= ventral length, Plat= proximal height Si= proximal spine length. Appendage in (b) from [31].

REFERENCES

1. Daley A.C., Edgecombe G.D. 2014 Morphology of *Anomalocaris canadensis* from the Burgess Shale. *Journal of Paleontology* **88**(1), 68-91. (doi:10.1666/13-067).
2. Daley A.C., Budd G.E., Caron J.-B. 2013 Morphology and systematics of the anomalocaridid arthropod Hurdia from the Middle Cambrian of British Columbia and Utah. *Journal of Systematic Palaeontology* **11**(7), 743-787. (doi:10.1080/14772019.2012.732723).
3. Moysiuk J., Caron J.-B. 2019 A new hurdiid radiodont from the Burgess Shale evinces the exploitation of Cambrian infaunal food sources. *Proceedings of the Royal Society B: Biological Sciences* **286**(1908), 20191079. (doi:doi:10.1098/rspb.2019.1079).
4. Whittington H.B., Briggs D.E.G. 1985 The largest Cambrian animal, *Anomalocaris*, Burgess Shale, British-Columbia. *Philosophical Transactions of the Royal Society of London B, Biological Sciences* **309**(1141), 569-609. (doi:10.1098/rstb.1985.0096).
5. DALEY A.C., BUDD G.E. 2010 New anomalocaridid appendages from the Burgess Shale, Canada. *Palaeontology* **53**(4), 721-738. (doi:https://doi.org/10.1111/j.1475-4983.2010.00955.x).
6. Briggs D.E.G. 1979 *Anomalocaris*, the largest known Cambrian arthropod. *Paleontology* **22**, 631-664.
7. Pates S., Daley A.C., Butterfield N.J. 2019 First report of paired ventral endites in a hurdiid radiodont. *Zoological Letters* **5**(1), 18. (doi:10.1186/s40851-019-0132-4).
8. Daley A.C., Budd G.E., Caron J.-B., Edgecombe G.D., Collins D. 2009 The Burgess Shale Anomalocaridid *Hurdia* and its significance for early Euarthropod evolution. *Science* **323**(5921), 1597-1600. (doi:10.1126/science.1169514).
9. Friedman M. 2012 Parallel evolutionary trajectories underlie the origin of giant suspension-feeding whales and bony fishes. *Proceedings of the Royal Society B: Biological Sciences* **279**(1730), 944-951. (doi:http://doi:10.1098/rspb.2011.1381).